Lxrα regulates the androgen response in prostate epithelium

Emilie Viennois, Teresa Esposito, Julie Dufour, Aurélien Pommier, Stéphane Fabre, Jean-Louis Kemeny, Laurent Guy, Laurent Morel, Jean-Marc A. Lobaccaro, Silvère Baron

Lxrα Regulates the Androgen Response in Prostate Epithelium

Emilie Viennois, Teresa Esposito, Julie Dufour, Aurélien Pommier, Stephane Fabre, Jean-Louis Kemeny, Laurent Guy, Laurent Morel, Jean-Marc Lobaccaro, and Silvère Baron

Department of Génétique Reproduction et Développement (E.V., T.E., J.D., A.P., L.M., J.-M.L., S.B.), Clermont Université, Université Blaise Pascal, and Centre de Recherche en Nutrition Humaine d'Auvergne (E.V., T.E., J.D., A.P., L.M., J.-M.L., S.B.), F-63000 Clermont-Ferrand, France; Centre National de la Recherche Scientifique, Unité Mixte de Recherche 6293 (E.V., T.E., J.D., A.P., L.M., J.-M.L., S.B.), and Institut National de la Santé et de la Recherche Médicale, Unité 1103 (E.V., T.E., J.D., A.P., L.M., J.-M.L., S.B.), GReD, F-63177 Aubiere, France; Dipartimento di Medicina Sperimentale (T.E.), Laboratorio di Biologia Molecolare, Section F. Bottazzi, Second University of Naples, F-80138 Naples, Italy; Department of Physiologie de la Reproduction et des Comportements (S.F.), Unité Mixte de Recherche 6175 Institut National de la Recherche Agronomique-Centre National de la Recherche Scientifique-Université de Tours-Haras Nationaux, F-37380 Nouzilly, France; and Service de Pathologie (J.-L.K.) and Service d'Urologie (L.G.), Hôpital Gabriel Montpied, F-63003 Clermont-Ferrand, France

Benign prostatic hyperplasia is a nonmalignant enlargement of the prostate that commonly occurs in older men. We show that liver X receptor (Lxr)-α knockout mice (*lxr*$\alpha^{-/-}$) develop ventral prostate hypertrophy, correlating with an overaccumulation of secreted proteins in prostatic ducts and an alteration of vesicular trafficking in epithelial cells. In the fluid of the *lxr*$\alpha^{-/-}$ prostates, spermine binding protein is highly accumulated and shows a 3000-fold increase of its mRNA. This overexpression is mediated by androgen hypersensitivity in *lxr*$\alpha^{-/-}$ mice, restricted to the ventral prostate. Generation of chimeric recombinant prostates demonstrates that Lxrα is involved in the establishment of the epithelial-mesenchymal interactions in the mouse prostate. Altogether these results point out the crucial role of Lxrα in the homeostasis of the ventral prostate and suggest *lxr*$\alpha^{-/-}$ mice may be a good model to investigate the molecular mechanisms of benign prostatic hyperplasia. (*Endocrinology* 153: 3211–3223, 2012)

Benign prostate hyperplasia (BPH) is a common disorder that affects 50% of 60-yr-old men (1) characterized by lower urinary tract disorders having severe effects on the quality of life. Three main forms of BPH have been described: glandular, fibrous, and muscular. Pharmacological treatment of BPH relies on two types of medications: 5α-reductase inhibitors, such as finasteride, which inhibit the conversion of testosterone into dihydrotestosterone (DHT) (2), and α-blockers, such as prazosin, which block the α-adrenergic receptor in the smooth muscle helping to relax prostate-associated muscle fibers (3). In addition to pharmacological treatment, transurethral prostate resection is the reference surgical procedure.

Androgens are important in prostate embryonic development as well as in the adult prostate (4), and androgen-mediated signaling plays a central role in the etiology of prostatic hypertrophy. Androgen receptor (AR; NR3C4) belongs to the nuclear hormone receptor superfamily and is activated by DHT or testosterone (5, 6). Interestingly, inhibition of testosterone conversion into DHT, the major active androgen within the prostate (7), is one of the most effective pharmacological treatments of BPH (2). Cunha (8) has extensively described the role of mesenchymal-epithelial interactions in normal and pathological prostate development as well as adult prostate homeostasis. Com-

ISSN Print 0013-7227 ISSN Online 1945-7170
Printed in U.S.A.

doi: 10.1210/en.2011-1996 Received November 16, 2011. Accepted April 5, 2012.
First Published Online April 30, 2012

Abbreviations: AR, Androgen receptor; BPH, benign prostate hyperplasia; DHT, dihydrotestosterone; EEA1, Early endosome antigen 1; IP, immunoprecipitation; LXR, liver X receptor; MEF, mouse embryonic fibroblast; MPE, mouse prostate epithelial; PMSF, phenylmethylsulfonyl fluoride; SBP, spermine binding protein; UGE, urogenital epithelia; UGM, urogenital mesenchyme; VP, ventral prostate; WT, wild type.

binations were made between mesenchymal and epithelial tissue derived from normal embryos or mice with the mutation *Tfm* (9) (testicular feminized) in AR, which inhibits its function and makes animals insensitive to androgens. Different combinations of urogenital mesenchyme (UGM) and urogenital epithelia (UGE) demonstrated that mesenchymal-epithelial interactions were necessary for prostate development. Moreover, AR signaling in epithelial cells is not sufficient for the morphological development of the prostate, whereas mesenchymal AR is necessary and sufficient. In addition, these experiments demonstrate the existence of paracrine factors synthesized by mesenchymal cells in response to androgens that regulate the function and survival of epithelial cells.

Recent studies identified liver X receptors (LXR) as factors involved in prostate physiology (reviewed in Ref. 10). LXRα (NR1H3) and LXRβ (NR1H2), two members of the nuclear receptor superfamily, are bound by oxidized forms of cholesterol known as oxysterols. Activated LXR stimulate expression of target genes involved in lipid metabolism (11, 12). Interestingly, LXR ligands such as synthetic T0901317 have antiproliferative effects on the prostate cancer cell line LNCaP (13). We have previously shown that LXR activation also leads to LNCaP cell death by apoptosis as well as inhibition of tumor growth in xenograft models (14). Moreover, LXR activity can be downregulated by AR in LNCaP cells at the promoter level (15). This regulation implies the involvement of the N-terminal domain of AR. Conversely, constitutive activation of *Lxrα* in the liver activates androgen catabolism in mice (16).

Kim *et al.* (17) demonstrated that *Lxrα*-deficient mice were characterized by several BPH-like features such as dilated prostatic ducts, hyperproliferative epithelium, and hypertrophic stroma. The authors suggested that this phenotype resulted from stromal compartment alterations but did not provide any mechanism to explain the BPH phenotype. Moreover, knowing the crucial role of androgens in prostate homeostasis, we hypothesized that this phenotype was in part due to alterations of androgen signaling. Neither the specific role of each compartment in phenotype establishment nor the specific role of the androgenic pathway has previously been investigated.

The aim of this study was to understand how Lxrα could be involved in prostate physiology and whether Lxrα could interfere with androgen signaling *in vivo*, which could account for the BPH-like phenotype in mice defective for this nuclear receptor.

Materials and Methods

Animal care and animal experiments procedure

Lxr-knockout mice [$lxr\alpha^{-/-}$, $lxr\beta^{-/-}$, and $lxr\alpha\beta^{-/-}$ (18)] and wild-type (WT) mice were maintained on a mixed strain background (C57BL/6:129Sv) and housed in a temperature-controlled room with 12-h light, 12-h dark cycles. They were fed *ad libitum* with water and Global-diet 2016S (Harlan, Gannat, France). Eight- to 12-month-old mice were anesthetized by ketamine/xylasine; blood was collected by cardiac puncture, whereupon animals were killed by cervical dislocation and organs harvested. Some mice were surgically castrated at 6 months of age. Three weeks after the surgical procedure, castrated mice received two daily im injections of 75 μg/kg testosterone propionate for 1 wk (Sigma-Aldrich; L'Isle d'Abeau, France) to allow the prostate to regenerate. Animals were then killed and the ventral prostate (VP) lobes were collected for various analyses. For antiandrogen experiments, 6-month-old mice were daily gavaged with the antiandrogen bicalutamide (12 mg/d/kg, Casodex; AstraZeneca, Rueil-Malmaison, France) or with vehicle methyl-cellulose. All the chemicals were from Sigma-Aldrich unless otherwise indicated. All mouse experiments were performed in agreement with the local ethic committee (no. CE26-11).

Anatomy and pathology analyses

VP lobes were collected, fixed in 4% PFA, and embedded in paraffin. Sections were stained with hematoxylin/eosin or Masson's trichrome and analyzed with an Axioplan 2 microscope (Carl Zeiss Vision GmbH, LePecq, France). For electron microscopy, samples were fixed in 2% glutaraldehyde-0.5% paraformaldehyde in cacodylate buffer at 4 C for 24 h. Fixed VP were subsequently postfixed for 1.5 h in buffered osmium tetraoxide at 4 C and embedded in Epon Araldite (Delta Microscopies, Ayguesvives, France). Ultrathin sections was stained with uranyl acetate and observed with a Hitachi H-7650 transmission electron microscope (Hitachi Elexience, Verrières-le-Buisson, France). Use of human samples was approved by the local ethical committee. Subjects received counseling and provided written consent for the study.

Mouse prostate epithelial cell establishment

The culture procedure was derived from methods developed for mouse vas deferens epithelial cells by Manin et *al.* (19). Briefly, mouse prostate epithelial (MPE) cells were harvested from the VP lobes of 20- to 30-d-old $lxr\alpha^{-/-}$ or WT mice and transferred onto cell culture insets (BD Falcon TM, Fontenay-sous-Bois, France) coated with a thin layer of extracellular matrix gel (Sigma Aldrich) and cultured in complete medium [DMEM/F12 (50:50; Invitrogen, Oslo, Norway) supplemented with 0.5% fetal bovine serum (Biowest, Nuaillé, France), cholera toxin (10 ng/ml), epidermal growth factor (5 ng/ml), gentamycin (100 μg/ml), insulin (5 μg/ml), transferrin (10 μg/ml), L-glutamine (2 mM), HEPES (20 mM), ethanolamine (0.6 μg/ml), cAMP (25 μg/ml), selenium (17.3 ng/ml), and hydrocortisone (10 nM)].

Cell immunofluorescence and lysosomal labeling

MPE were fixed in 4% paraformaldehyde and permeabilized in PBS Triton X-100 0.1%. Detection were performed using antirabbit EEA1 (Abcam, Paris, France) and antimouse tubulin (BD Transduction Laboratories, Le Pont de Claix, France) antibodies and revealed with Alexa 488-conjugated antirabbit and Alexa 555-conjugated antimouse immunoglobulins (Invitrogen). For lysosomal analysis, MPE were incubated in minimal medium containing 50 mM of lysotrackerRed (Invitrogen).

Cell culture and transient transfection

Mouse embryonic fibroblast (MEF) were transfected 24 h after seeding with 1 μg of the luciferase reporter construct ARE-TK-LUC (20) in combination with 500 ng or 1 μg of pSG5-hAR using Lipofectamine 2000 (Sigma-Aldrich). After transfection, cells were starved for 12 h in a basal medium without growth factors and were then cultured in DMEM in the absence or the presence of 1 nM DHT (Sigma-Aldrich) for 24 h. Luciferase activity was measured using luciferase assay kit (Promega, Charbonnières-les-Bains, France).

Hormone measurement

Plasma testosterone was extracted with ethyl acetate-cyclohexane as previously described (21) and measured by RIA. The limit of detection of the testosterone assay was 6 pg/tube, and the intraassay coefficient of variation was less than 12%. The antiserum cross-reacted with 5α-dihydrotestosterone (65%), 5β-dihydrotestosterone (49.5%), androstenedione (0.7%), and less so with other steroids (<0.1%).

Intraprostatic DHT was quantified using an enzymatic immunoassay kit from Diagnostics Biochem Canada Inc. (London, Canada) (22). Briefly, ventral prostate lobes were homogenized with tissue lyser (QIAGEN, Les Ulis, France) in a solution of PBS-0.1 mg/ml BSA. DHT concentration in the homogenate was determined according to the manufacturer's instructions.

Quantitative PCR

mRNA were extracted using the NucleoSpin RNA II kit (Macherey Nagel EURL, Hoerdt, France). cDNA was synthesized with 200 U of Moloney murine leukemia virus-reverse transcriptase (Promega), 5 pmol of random primers (Promega), 40 U RNAsin (Promega), and 2.5 mM deoxynucleotide triphosphate. Quantitative PCR was performed on a Mastercycler ep Realplex (Eppendorf, LePecq, France) using MESA GREEN quantitative PCR masterMix Plus for SYBR (Eurogentec, Angers, France). Sequences of the primers used are listed in Supplemental Fig. 1, published on The Endocrine Society's Journals Online web site at http://endo.endojournals.org.

Coomassie blue gel and liquid chromatography and tandem mass spectrometry analysis

Proteins were extracted using HEPES 20 mM, NaCl 0.42 M, $MgCl_2$ 1.5 mM, EDTA 0.2 mM, and Nonidet P-40 1% supplemented with phenylmethylsulfonyl fluoride (PMSF) 1 mM (Sigma-Aldrich), protease inhibitor (Complete 1X; Roche Molecular Biochemicals, Meylan, France), NaF 0.1 mM, and Na_2VO_3 0.1 mM (Sigma-Aldrich). Total proteins were loaded on Mini-PROTEAN TGX 4–15% precast gels (Bio-Rad Laboratories, Marnes la Coquette, France), and gels were stained with Coomassie brilliant blue G-250 (Bio-Rad Laboratories). Protein bands were excised, destained, and submitted to tryptic digestion, as previously described (23). Briefly, positive ion matrix-assisted laser desorption ionization mass spectra were recorded in the reflectron mode of a matrix-assisted laser desorption ionization-time of flight-mass spectrometry (Voyager DE-Pro; Applied Biosystems, Carlsbad, CA). The *Mus musculus* Swissprot database was queried using Mascot software. The following parameters were considered for the searches: a maximum ion mass tolerance of ±25 ppm, partial oxidation of methionine, and one maximum miss cleavage.

Western blot analysis

Total proteins were subjected to denaturing SDS-PAGE and transferred to nitrocellulose Hybond-ECL membrane (GE Healthcare Life Sciences, Velizy-Villacoublay, France). Detections were performed using antibodies raised against β-actin (Sigma-Aldrich), AR (PG21; Millipore, Euromedex, Mundolsheim, France), or pan-prostate secretions (a kind gift from Dr. C. Abate-Shen, Department of Medicine, Columbia University Medical Center, New York, NY) and revealed with peroxidase-conjugated antirabbit IgG (P.A.R.I.S, Compiègne, France) using a Western Lightning System kit (PerkinElmer, Villebon sur Yvette, France).

Chromatin immunoprecipitation

Ventral prostates were harvested and homogenized in 200 μl of cell lysis buffer (5 mM 1,4-piperazine diethane sulfonic acid PIPES, 85 mM KCl, 0.5% Nonidet P-40) supplemented with PMSF 1 mM, and protease inhibitors one time. After centrifugation chromatin complexes were fixed by 1% formaldehyde/PBS for 15 min at room temperature. Fixation was stopped by the addition of glycine (125 mM final). After centrifugation, pellets were washed twice in PBS supplemented with 1 mM PMSF and protease inhibitors. Nuclei were then lysed 45 min on ice in nucleus lysis buffer [50 mM Tris-HCl (pH 8.0), 10 mM EDTA, 1% sodium dodecyl sulfate], and chromatin was sheared by sonication. Chromatin was then precleared 2 h at 4 C in 500 μl immunoprecipitation (IP) buffer [0.01% sodium dodecyl sulfate, 1.1% Triton X-100, 1.2 mM EDTA, 16.7 mM Tris-HCl (pH 8.1) and 167 mM NaCl] containing 30 μl of Dynabeads Protein A (Invitrogen). The beads were subsequently discarded with MagnaRack (Invitrogen) and the sample was split in two identical fractions. Immunoprecipitation was performed overnight at 4 C with 5 μg of negative control IgG (Diagenode, Liège, Belgium) or specific anti-AR antibody (Millipore). Beads were washed six times in cold IP buffer and elutions were performed according to Chelex protocol (Bio-Rad Laboratories). Before PCR, chromatin samples were further purified using Qiaquick PCR purification columns (QIAGEN) and eluted in 30 μl of water. PCR was performed on 2 μl of eluted chromatin using GoTaq (Promega).

PCR was performed with the following primers: *fkbp5*, 5′-ACCCCCATTTTAATCGGAGAAC-3′ and 5′-TTTTGAAG AGCACAGAACACCCT-3′;*sbp*,5′-GCCCCTACTGACCCAG TATAGC-3′ and 5′-GAACTTTGTTTTCTGCTTATCCCT CAG-3′; and *pbsn*, 5′-ATACTAAATGACACAATGTCAA TG-3′ and 5′-CCCCAACACATTTGTTATTCTC-3′. The targeted androgen-responsive element-containing sequences for the *sbp* and *fkbp5* promoters were designed as previously described (24, 25).

Urogenital sinus dissection and subrenal prostate regeneration

Urogenital sinuses were collected from embryonic d 16.5 embryos and dissected into UGE and UGM as previously described (26). Briefly, dissected tissues were carefully digested with 10% trypsin at 4 C for 60 min and subsequent digestion with deoxyribonuclease (10 mg/ml; Roche). After 5 min, digestion was stopped with dissecting media (DMEM supplemented with 10% fetal bovine serum, penicillin-streptomycin, and glutamine; Invitrogen). The mesenchyme (UGM) was separated from the epithelium (UGE). Mesenchymes and epithelia were mixed in type

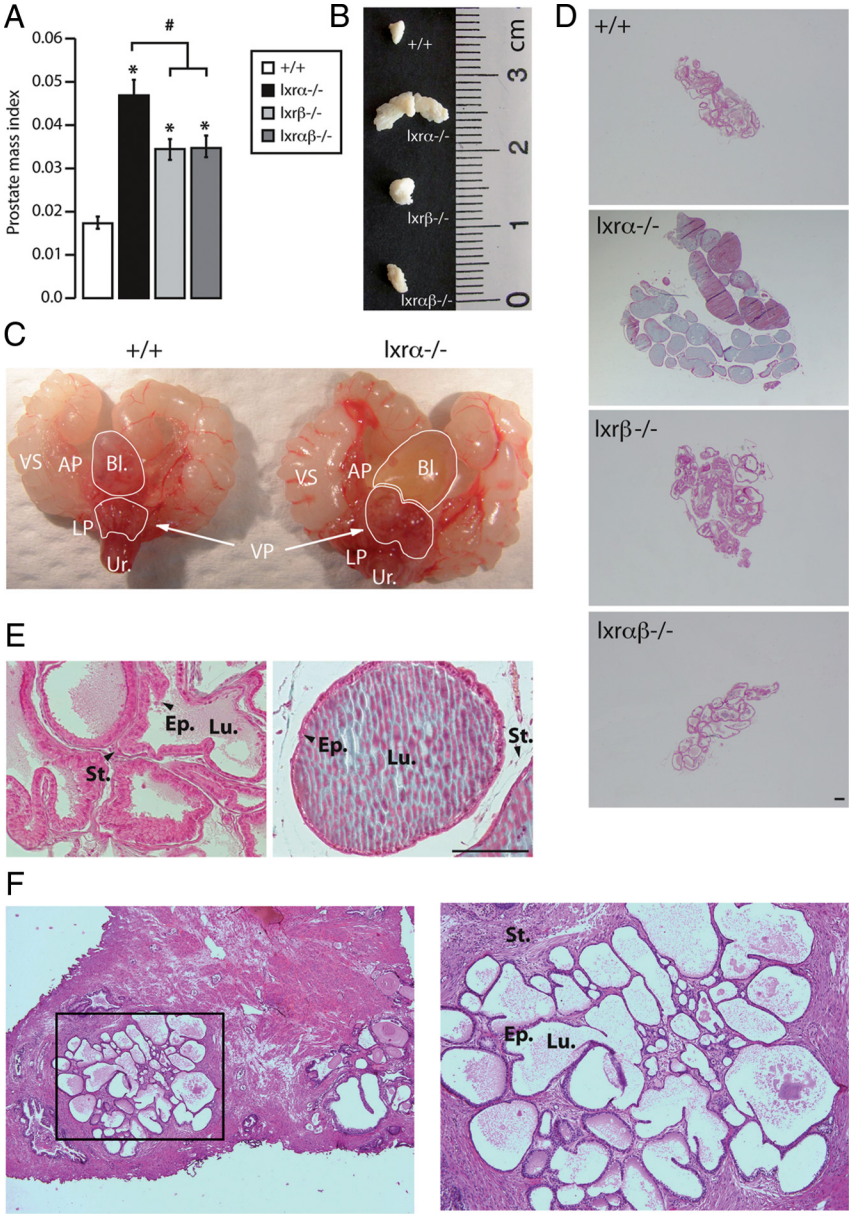

FIG. 1. *lxrα*$^{-/-}$ mice develop prostate hypertrophy. A, VP weight normalized to body weight of 12-month-old WT, *lxrα*$^{-/-}$, *lxrβ*$^{-/-}$, and *lxrαβ*$^{-/-}$ mice. *, $P < 0.05$ compared with the WT mice; #, $P < 0.05$ compared with *lxrα*$^{-/-}$ mice. B, Macroscopic observation of VP lobes after necropsy (size in centimeters). Both VP weight and size are increased in *lxrα*$^{-/-}$ mice compared with WT, *lxrβ*$^{-/-}$, and *lxrαβ*$^{-/-}$ mice (n = 17–26 for each genotype). C, Macroscopic urogenital tract pictures of *lxrα*$^{-/-}$ compared with WT mice. *Lxrα*$^{-/-}$ mice develop a bladder enlargement with urine accumulation. D and E, Masson trichrome staining of WT, *lxrα*$^{-/-}$, *lxrβ* $^{-/-}$, and *lxrαβ*$^{-/-}$ VP, at the age of 8 months. *Bars*, 200 μm. F, Hematoxylin-eosin staining of human prostate that exhibits the duct enlargement frequently observed in BPH patients. Bl, Bladder; LP, lateral prostate; VS, seminal vesicle; AP, anterior prostate; Ur, urethra; Ep, epithelium; Lu, lumen; St, stroma.

1 collagen prepared extemporaneously (collagen, NaOH 1N; BD Biosciences). Four recombinations were generated: UGE_{WT}/UGM_{WT}; $UGE_{lxr\alpha-/-}$/$UGM_{lxr\alpha-/-}$; UGE_{WT}/$UGM_{lxr\alpha-/-}$; and $UGE_{lxr\alpha-/-}$/UGM_{WT}. After collagen polymerization at 37 C, the recombinants were cultured at 37 C, 5% CO_2 in dissecting media supplemented with 10^{-7} M DHT (Sigma-Aldrich) for 24 h before grafting under the kidney capsule in anesthetized male nude mice (Charles River, L'Arbresle, France) (26, 27). After kidney repositioning, mice were sutured. The grafts were harvested 8 wk after surgery. All mouse experiments were performed in agreement with the local ethic committee (no. CE21-11).

Statistical analysis

Values are expressed as means ± SEM. Statistical comparisons were performed using a two-tailed Student's *t* test. A $P < 0.05$ was considered statistically significant.

Results

Mice lacking Lxrα develop BPH-like features associated with abnormal epithelial secretory activity

VP were obtained from 12-month-old WT, *lxrα*$^{-/-}$, *lxrβ*$^{-/-}$, and *lxrαβ*$^{-/-}$ mice. Lobe weights (Fig. 1A) and sizes (Fig. 1B) were significantly higher in *lxr*$^{-/-}$ compared with WT mice. *Lxrα*$^{-/-}$ mice had the most prominent phenotype with a 2.7-fold weight increase compared with WT (*vs.* 2-fold for *lxrβ*$^{-/-}$ and *lxrαβ*$^{-/-}$ mice). Therefore, most of the subsequent experiments were carried out using the *lxrα*$^{-/-}$genotype. Macroscopic analysis (Fig. 1C) showed that *lxrα* $^{-/-}$ mice had urine-filled bladders, a sign of urinary flow obstruction usually observed in BPH patients. Histological analysis showed that prostatic ducts were aberrantly dilated (Fig. 1, D and E) and filled up with large amounts of secretion fluid, which could account for the increase in VP weight. Interestingly, this phenotype was restricted to VP (Supplemental Fig. 2A). These histological features are similar to dilated glands observed in some BPH patients (Fig. 1F). However, no evidence of fibrous nodule formation was found in our cohort as previously described (17). Altogether these observations suggested that the enlarged VP phenotype could result from the deregulation of epithelial secretion activity. To further evaluate a potential secretory phenotype, VP tissue sections were analyzed by electron microscopy. These experiments showed larger secretion vesicles (Fig. 2, D and E) filled with a filamentous content (Fig. 2F) in the cytoplasm of *lxrα*$^{-/-}$ VP cells com-

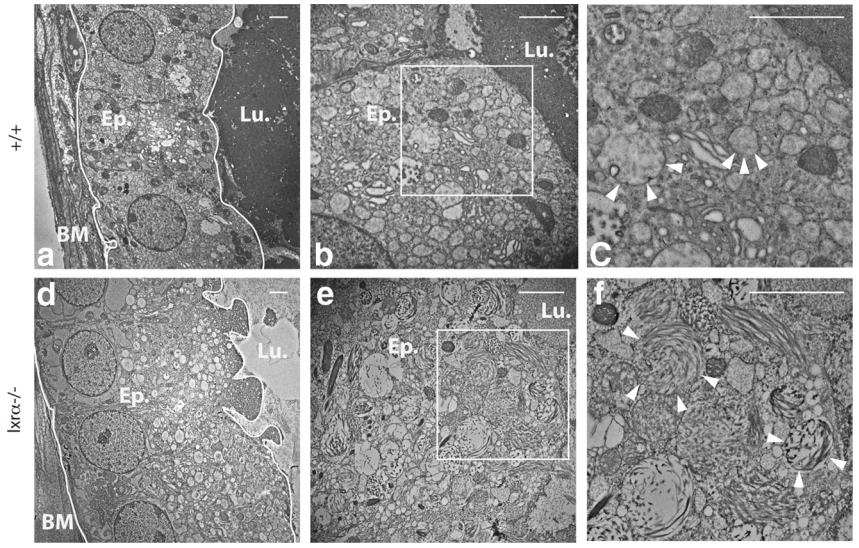

FIG. 2. Lxrα-deficient mice present an abnormal epithelial secretory activity. Ultrathin sections of VP from WT (A–C) or *lxr*$\alpha^{-/-}$ (D–F) mice were made and analyzed by electron microscopy to observe the ultrastructural organization of the cells within the cytoplasm. *White arrowheads* indicate secretory vesicles. These are bigger and present filamentous content in cytoplasm of *lxr*$\alpha^{-/-}$ epithelial cells. Ep, Epithelium; Lu, lumen; BM, basal membrane. *Bar*, 2 μm. *Squared portions* indicate the magnified view shown in C and F.

pared with WT (Fig. 2, A–C). Interestingly, this phenotype was not observed in *lxr*$\beta^{-/-}$ VP (data not shown), even though the LXRβ isoform is expressed (Supplemental Fig. 2B). There is no compensation of *lxr* isoform expression in each genotype (Supplemental Fig. 2C). Altogether these data suggested that there were an abnormal vesicle trafficking and vesicle structures in the VP of *lxr*$\alpha^{-/-}$ mice.

Vesicular trafficking is altered in epithelial cells derived from *lxr*$\alpha^{-/-}$ ventral prostate

To investigate the intrinsic role of Lxrα in VP epithelium, vesicular trafficking was analyzed in MPE cells derived from the VP of *lxr*$\alpha^{-/-}$ or WT mice. Expression of Early endosome antigen 1 (EEA1), a protein that binds phospholipid vesicles and is involved in endosomal trafficking, was analyzed. Immunolabeling of tubulin was used to assess cellular morphology and all trafficking apparatus integrity. We found that endosomal vesicles were smaller in *lxr*$\alpha^{-/-}$ MPE compared with WT (Fig. 3, Ac and Af). Lysosome biogenesis is tightly linked to vesicle trafficking (28). Therefore, we analyzed the effect of Lxrα ablation on lysosome structure by incubation of MPE cells with Lysotracker (Invitrogen). These experiments showed that lysosomes were smaller and less abundant in *lxr*$\alpha^{-/-}$ *vs.* WT MPE (Fig. 3, Ai and Al). Taken together, these observations show that the absence of Lxrα in ventral prostate epithelial cells results in abnormal vesicle trafficking and reduced lysosome biogenesis. Next we sought to ascertain whether the VP of mice lacking *lxr*α and/or *lxr*β exhibited deregulated expression of genes involved in cell trafficking (Fig. 3B). We observed that *syngr*, *lamp1*, *golgb1*, and *rab27b* expressions were up-regulated in *lxr*$\alpha\beta^{-/-}$ mice and *synpr* expression was down-regulated in *lxr*$\alpha^{-/-}$, *lxr*$\beta^{-/-}$, and *lxr*$\alpha\beta^{-/-}$ mice (Fig. 3C). Altogether these results demonstrated that Lxrα and Lxrβ are required for a normal trafficking and secretory machinery in prostatic epithelium.

Lxr$\alpha^{-/-}$ ventral prostate exhibits an overaccumulation of secreted spermine binding protein (SBP) in the prostatic fluid

To decipher the molecular mechanisms leading to the phenotype observed in VP from *lxr*$\alpha^{-/-}$ mice, protein accumulation profiles were analyzed by Western blotting followed by protein identification by mass spectrometry. Coomassie blue staining showed that Lxrα ablation resulted in multiple alterations in overall protein content (Fig. 4A). These observations were confirmed by Western blot using an antiserum directed toward the whole secretory content of mouse prostatic fluid (29) in isolated secretions and in cell lysates from WT and *lxr*$\alpha^{-/-}$ mice (Fig. 4B). Both experiments showed strong accumulation of a 30-kDa protein in WT samples (band 1). This signal was absent from *lxr*$\alpha^{-/-}$ samples. However, these samples were characterized by the strong accumulation of a 22/25 kDa protein (band 2) (Fig. 4B). Surprisingly, mass spectrometry analysis showed that both bands contained the same protein identified as SBP (Fig. 4C). The molecular weight discrepancy could result from differential posttranslational modifications. Indeed, SBP is known to be a highly glycosylated protein, which can be detected at multiple molecular weights (30). We further investigated the mechanisms of SBP deregulation by analyzing *sbp* expression using quantitative RT-PCR. This showed that *sbp* mRNA accumulation (Fig. 4D) was increased 3000-fold in *lxr*$\alpha^{-/-}$ VP, suggesting that Lxrα ablation affects *Sbp* gene transcription. It is also noteworthy that *sbp* expression presents a discrete deregulation in *lxr*$\beta^{-/-}$ mice and no alteration in *lxr*$\alpha\beta^{-/-}$ mice (Fig. 4D). Given that *lxr*$\alpha^{-/-}$ mice exhibit an increased enlargement of VP lobe compared with *lxr*$\beta^{-/-}$ and *lxr*$\alpha\beta^{-/-}$ mice and that SBP overaccumulation is observed only in *lxr*$\alpha^{-/-}$ prostatic fluid (data not shown), we can conclude that *sbp* gene deregulation plays a central role in the prostate phenotype of *lxr*$\alpha^{-/-}$ mice.

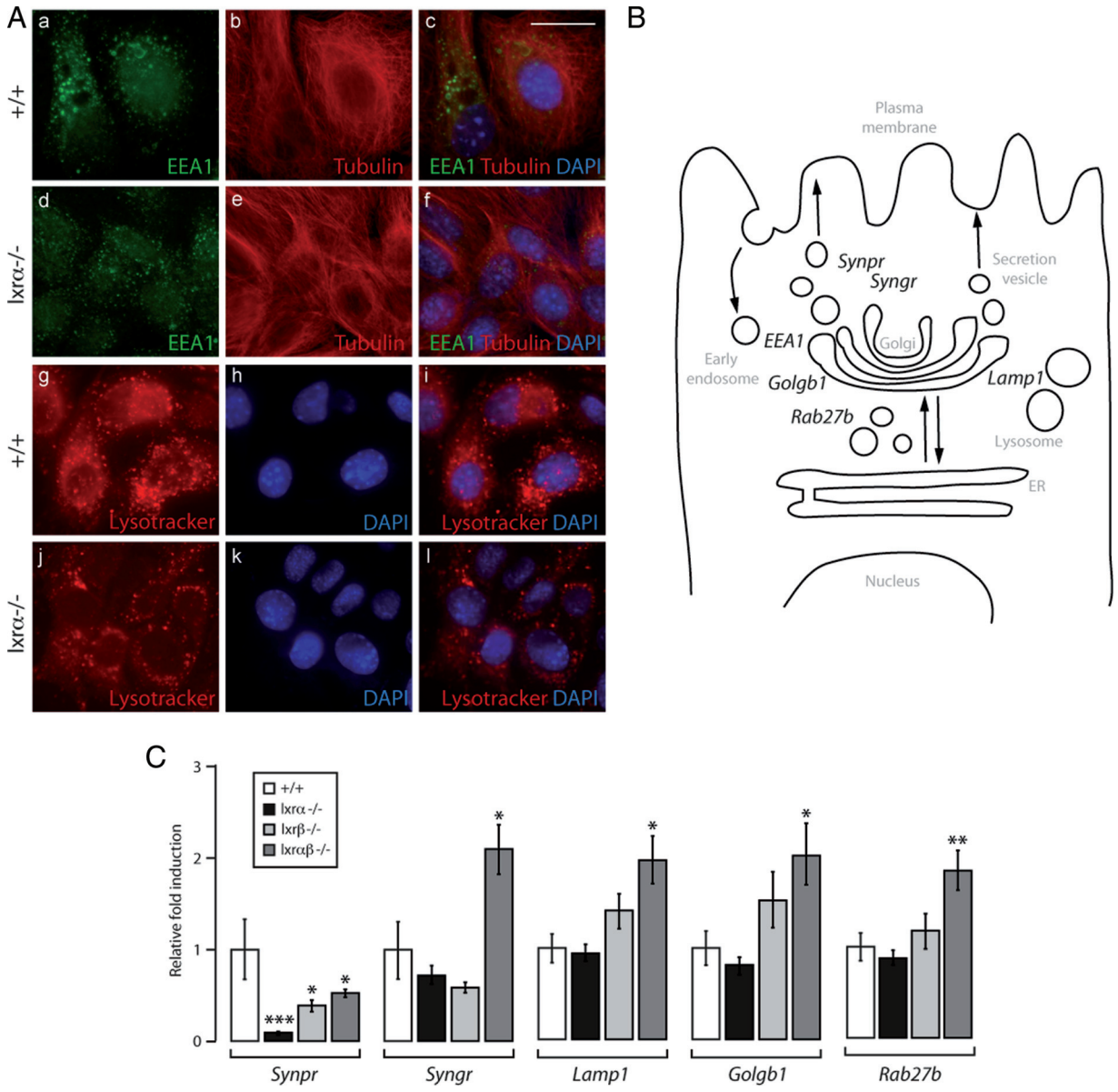

FIG. 3. Vesicular trafficking is altered by Lxr ablation. A, WT and *lxrα*$^{-/-}$ MPE were immunostained using anti-EEA1 (a and d) and antitubulin (b and e) antibodies. The EEA1 labeling demonstrated that endosomal vesicles were smaller in *lxrα*$^{-/-}$ *vs.* WT. Lysotracker analysis (g, i, j, and l; Invitrogen) was performed in MPE cells. Cell nuclei were stained with Hoechst. Lysotracker analysis showed that lysosomes were smaller and less abundant in *lxrα*$^{-/-}$ *vs.* WT. *Bar*, 20 μm. B, Schematic representation of the main proteins involved in secretion machinery in epithelial cells. Eea1, Early endosome antigen 1; Synpr, synaptoporin; Syngr, synaptogyrin; Lamp1, lysosomal-associated membrane protein 1; Golgb1, golgin B1; Rab27b, RAS oncogene family. C, mRNA relative accumulation levels of *synpr1*, *syngr*, *lamp1*, *golgb1*, and *rab27b* was measured in 9- to 12-month-old animals by quantitative PCR and normalized using *18s* (n = 7–10). *, $P < 0.05$, **, $P < 0.01$ compared with WT.

Sbp over accumulation in *lxrα*$^{-/-}$ mice is mediated by androgens

SBP is the most abundant protein within the prostatic fluid and its accumulation is tightly regulated by androgens (24, 31). To investigate whether the higher accumulation of SBP in the VP of *lxrα*$^{-/-}$ mice resulted from increased levels of androgens, the plasma testosterone level was evaluated. As shown in Fig. 5A, plasma testosterone was significantly increased by 2-fold in Lxrα-lacking mice compared with WT. The increased circulating testosterone level can be explained by the increase of *sts* (steroid sulfatase), a mRNA-encoding enzyme that converts sulfoned androgens into active metabolites in both the liver and VP. In contrast, *sult2a1* (sulfotransferase 2a1) was undetectable in the VP and its expression was unaltered in the liver (Supplemental Fig. 3) (16). Even though testosterone was higher in *lxrα*$^{-/-}$ mice, the concentration of DHT, the active androgen in the prostate, was not significantly altered by Lxrα ablation (Fig. 5A). Likewise, AR protein accumulation was not altered in the VP of *lxrα*$^{-/-}$ mice (Fig. 5B). We thus concluded that increased ligand production or receptor expression was

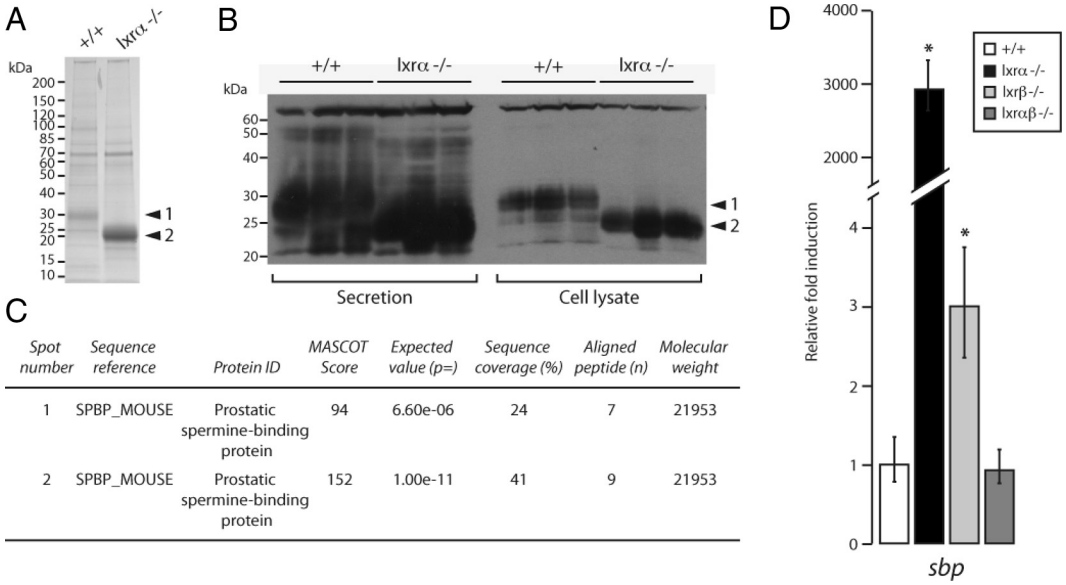

C

Spot number	Sequence reference	Protein ID	MASCOT Score	Expected value (p=)	Sequence coverage (%)	Aligned peptide (n)	Molecular weight
1	SPBP_MOUSE	Prostatic spermine-binding protein	94	6.60e-06	24	7	21953
2	SPBP_MOUSE	Prostatic spermine-binding protein	152	1.00e-11	41	9	21953

FIG. 4. *Lxrα*$^{-/-}$ ventral prostate exhibits an overaccumulation of the secreted protein SBP. A, Secretion protein lysates of WT and *lxrα*$^{-/-}$ ventral prostates were resolved using 4–15% SDS-PAGE migration and the gel was stained with Coomassie Blue. B, Western blot analysis using antiprostate secretory protein immune serum was performed on samples of whole-prostate protein extracts or on prostate secretion only, from WT or *lxrα*$^{-/-}$ mice. C, The protein spots (*arrows 1 and 2* in A) were excised from the gel (A) and analyzed by mass spectrometry, and SBP protein was identified and found to be highly accumulated in secretions from *lxrα*$^{-/-}$ VP compared with WT. D, mRNA relative accumulation levels of *sbp* were measured in 9- to 12-month WT, *lxrα*$^{-/-}$, *lxrβ*$^{-/-}$, and *lxαrβ*$^{-/-}$ animals by quantitative PCR and normalized using *18s*. *Sbp* expression was 3000-fold higher in *lxrα*$^{-/-}$ VP compared with WT and is 3-fold higher in *lxrβ*$^{-/-}$ compared with WT. *Sbp* transcript accumulation remains unchanged in *lxrαβ*$^{-/-}$ compared with WT (n = 7–10). *, $P < 0.05$, ***, $P < 0.001$ compared with WT.

unlikely to account for the huge increase in s*bp* expression resulting from Lxrα ablation.

We then analyzed whether the increase in *sbp* expression in *lxrα*$^{-/-}$ VP was directly dependent on androgens by performing castration and testosterone complementation experiments (Supplemental Fig. 4). As expected, castration abolished *sbp* accumulation in the VP of WT mice (Fig. 5C, *white bars*). The same drastic decrease was observed in *lxrα*$^{-/-}$ mice, although the reduction was not as pronounced as in WT mice. Interestingly, testosterone treatment restored *sbp* expression in both WT and *lxrα*$^{-/-}$ castrated-mice (Fig. 5C, *black bars*), confirming that *sbp* expression was regulated by androgens in both genotypes. Careful examination of these data showed that *sbp* accumulation was much higher after testosterone propionate treatment in *lxrα*$^{-/-}$ mice (439-fold induction) compared with WT (122-fold induction). Furthermore, pharmacological inhibition of AR by the antiandrogen bicalutamide (Fig. 5D) resulted in decreased accumulation of *sbp* transcript both in WT (1.69-fold inhibition) and *lxrα*$^{-/-}$ mice (2.78-fold inhibition). However, *sbp* accumulation was still higher in *lxrα*$^{-/-}$ than in WT VP after bicalutamide treatment. Castration, testosterone supplementation, and bicalutamide treatment were validated by histology analysis and prostate weight measurement (Supplemental Fig. 4). Altogether these data show that even though androgens are clearly involved in the regulation of *sbp* expression in VP of *lxrα*$^{-/-}$ mice, these mice still express higher amounts of *sbp* upon total androgen depletion (castration) or when AR is blocked (bicalutamide). We thus concluded that *sbp* accumulation *per se* was hypersensitive to androgens in *lxrα*$^{-/-}$ mice.

Basal *sbp* accumulation was significantly higher in castrated *lxrα*$^{-/-}$ than in WT mice (Fig. 5C). Some *Lxr* target genes show increased expression in *Lxr*-knockout mice in the absence of oxysterol stimulation such as *star* in the adrenal gland (18). This suggested that *sbp* could be a *bona fide* Lxrα target gene. To test this hypothesis, WT mice were gavaged short-term with T0901317, a synthetic LXR agonist. Neither alteration of *sbp* level nor other androgen target genes such as *fkbp5* and *pbsn* were seen in T0901317-gavaged mice (Supplemental Fig. 5), ruling out a direct regulation of *sbp* expression by Lxrα. These observations suggest that Lxrα indirectly affects basal *sbp* expression, resulting in increased androgen sensitivity.

Androgen hypersensitivity in *lxrα*$^{-/-}$ mice targets specific genes and is restricted to the VP

Next, we sought to determine whether the abnormal androgen response was VP specific or was also present in other tissues. Protein accumulation profiles were analyzed in several androgen-dependent tissues of the genital tract: dorsolateral and anterior prostates, epididymis, testis, vas

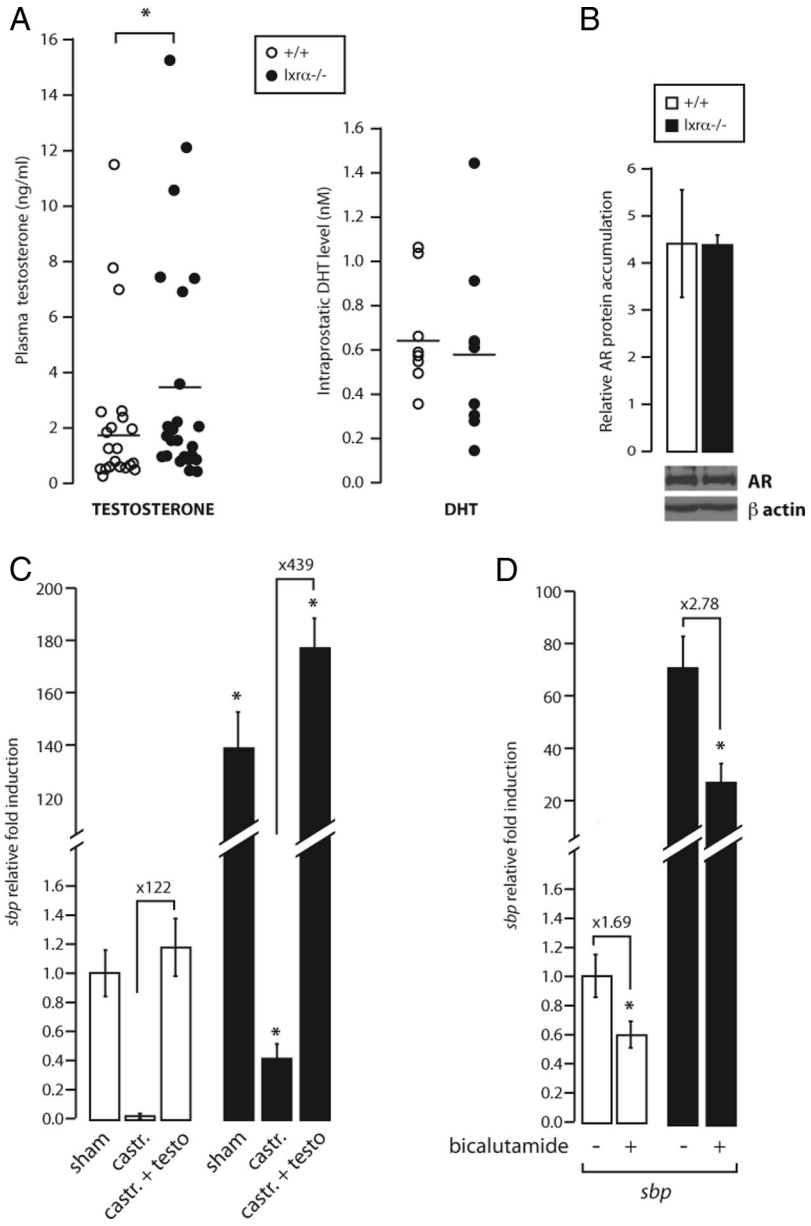

FIG. 5. *Sbp* expression deregulation in *lxrα*$^{-/-}$ mice is mediated by androgens. A, Testosterone concentrations were measured in the plasma of WT and *lxrα*$^{-/-}$ mice. Circulating testosterone was significantly increased in *lxrα*$^{-/-}$ (n = 25) compared with WT (n = 25) mice. The active androgen metabolite, DHT, was measured in the VP of WT and *lxrα*$^{-/-}$ mice. DHT levels were unchanged in the ventral prostate (n = 25). B, Basal AR accumulation determined by Western blot. As observed, this accumulation is unchanged in *lxrα*$^{-/-}$ VP. *, $P < 0.05$. C, *Sbp* accumulation in 5- to 6-month-old WT or *lxrα*$^{-/-}$ castrated (castr.) mice. Three weeks after castration, castrated mice were injected with 75 μg/kg of testosterone (testo) twice a day for 1 wk. Castration caused a large decrease of *sbp* in WT and *lxrα*$^{-/-}$ mice. Testosterone injection led to a larger recovery of *sbp* expression in the VP of *lxrα*$^{-/-}$ compared with WT mice, suggesting an androgen hypersensitivity in *lxrα*$^{-/-}$ (n = 7). *, $P < 0.05$ compared with sham WT mice. D, Five- to 6-month-old WT and *lxrα*$^{-/-}$ mice were treated with bicalutamide at a daily oral dose of 12 mg/kg for 21 d. Bicalutamide caused a 2.78-fold decrease of androgen-dependent *sbp* expression in *lxrα*$^{-/-}$ mice (1.69-fold decreased in WT mice) (n = 7–9). *, $P < 0.05$ compared with vehicle.

deferens, and seminal vesicles. There was no clear difference between the migration profiles of WT and *lxrα*$^{-/-}$ samples (Fig. 6A). This provided evidence that the abnormal response to androgens was restricted to the VP. We next investigated whether *sbp* was the only androgen-regulated gene to have its expression altered in the VP by analyzing the expression of several androgen-regulated genes by quantitative RT-PCR. These included *svs2* (seminal vesicle secretion-2) (32), *spp1* (secretory prostatic protein-1) (33), *fkbp5* (fk506 binding protein prostate-5) (25), *acpp* (acid phosphatase, prostate protein) (34), *calR* (calreticulin) (35), and *pbsn* (probasin) (36). Analysis of the PCR data allowed stratification of the genes into distinct categories (Fig. 6B): genes with increased basal expression (*svs2* and *spp1*); genes with unaltered expression (*fkbp5*, *acpp* and *calR*); and *pbsn* whose basal accumulation was significantly decreased by Lxrα ablation.

To gain insight into the molecular mechanisms accounting for these discrepancies, AR recruitment on the promoters of these genes was analyzed by *in vivo* chromatin immunoprecipitation. Surprisingly, the recruitment of AR to androgen-responsive element sequences of *sbp*, *pbsn*, and *fkbp5* promoters was unaltered by ablation of Lxrα (Fig. 6, C and D, and Supplemental Fig. 6). The similar recruitment of AR on target promoters in both WT and knockout VP suggested that Lxrα could act through an indirect route to modulate intrinsic AR transcriptional activity.

To test this hypothesis, WT and *lxrα*$^{-/-}$ MEF were transfected with the androgen-sensitive construct AREtk-Luc in the presence or absence of an AR expression vector (Fig. 6E). As expected, Lxrα was present and functional in WT MEF cells (data not shown). Treatment with DHT in the absence of AR transfection induced a moderate increase in activity of the androgen-sensitive luciferase reporter construct (1.6 fold) in WT MEF. This mild induction was not found in *lxrα*$^{-/-}$ MEF. As expected, androgen-responsiveness of the construct was further increased to 12-fold after AR transfection in WT cells. Surprisingly, there was no alteration of androgen responsiveness in *lxrα*$^{-/-}$ MEF upon AR transfection. This suggested that Lxrα did not directly alter intrinsic AR transcriptional efficiency.

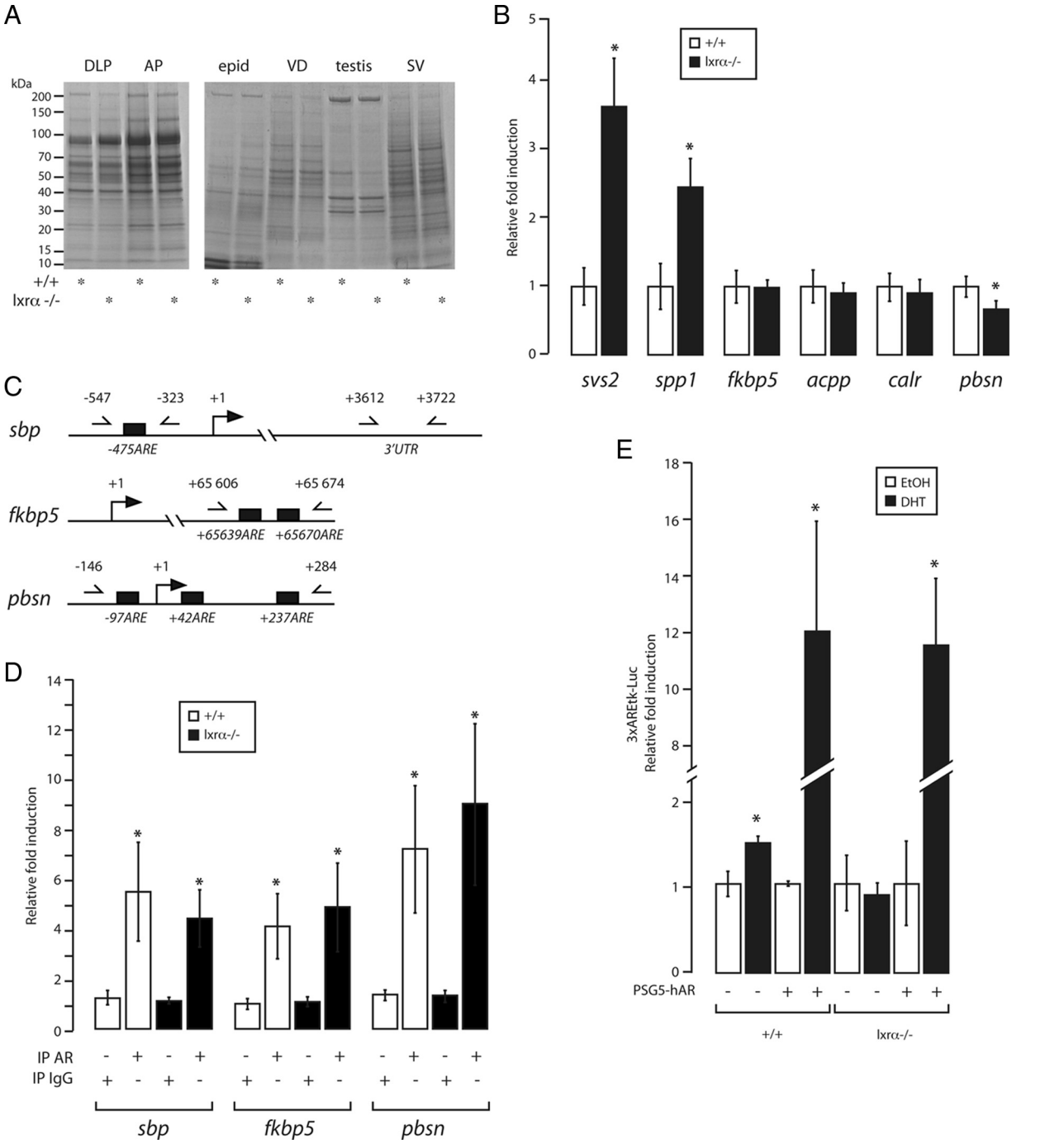

FIG. 6. Androgen hypersensitivity in *lxrα*$^{-/-}$ mice targets specific genes and is restricted to the VP. A, Whole-protein extracts from the dorsolateral and anterior prostate, epididymis, vas deferens, testis, and seminal vesicles were migrated in a 4–15% polyacrylamide gel and stained with Coomassie blue. The *sbp* accumulation is lobe specific and is not found in the other male genital tract tissues. B, mRNA relative accumulation levels of *svs2*, *spp1*, *fkbp5*, *acpp*, *calR*, and *pbsn* were measured by quantitative PCR and normalized with *18s* in the VP of intact WT mice. Some of them have the same accumulation profile as *sbp*, and others are down-regulated or remain unchanged in the VP (n = 7–10). *, $P < 0.05$ compared with the WT animals. C, Schematic representation of the androgen-responsive element regulatory sites on *sbp*, *fkbp5*, and *pbsn* promoter sequences. The figure shows the amplified regions. *Arrows* represent primer localization around the amplified regions. D, Anti-AR or anti-IgG chromatin immunoprecipitation was performed on the VP of WT and *lxrα*$^{-/-}$ mice. The AR specifically binds the regulatory element of androgen-regulated genes (*sbp*, *pbsn*, and *fkbp5*). Chromatin enrichment was quantified by quantitative PCR (n = 6–8 analyzed for three independent experiments). Lack of Lxrα does not modify AR recruitment on regulating regions. E, *Lxrα*$^{-/-}$ and WT MEF cells were transfected with the luciferase reporter construct ARE-tk-LUC in combination with pSG5-hAR and treated or not with 10^{-9} M DHT (means ± SEM). *, $P < 0.05$ compared with the respective excipient incubated cells. DLP, Dorsolateral prostate; AP, anterior prostate; epid, epididymes; VD, vas deferens; SV, seminal vesicle.

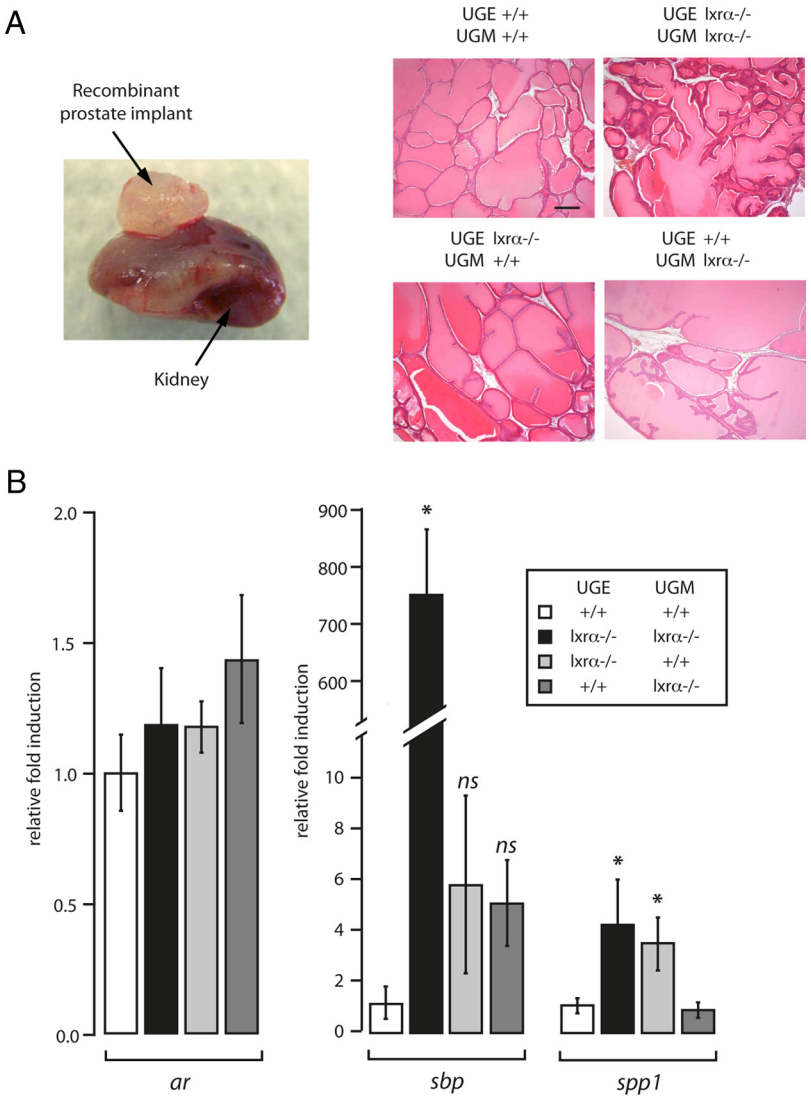

FIG. 7. The deregulation of androgen-dependent genes is dependent on both the stromal and epithelial compartments in *lxrα*$^{-/-}$ mice. A, UGE and UGM were dissected from WT or *lxrα*$^{-/-}$ embryos. Different combinations were performed (see text for more details). The different explants were grafted under the kidney capsule of nude mice. After 8 wk of growth, recombinant prostates (*left panel*) were dissected. Histological analysis (hematoxylin-eosin staining) was performed on the four different combinations (*right panel*). *Bar*, 200 μm. B, Accumulations of *ar*, *sbp*, and *spp1* mRNA were measured by quantitative PCR and the fold induction between each recombinant condition was represented (n = 3–7). *, $P < 0.05$ compared with the UGE_{WT}/UGM_{WT} condition.

Lxrα coordinates stroma/epithelium functions to control the androgen-dependent secretory activity of the ventral prostate in mice

Androgen action on the prostate is the result of a complex paracrine network between stromal cells and epithelium (8). Integration of androgen signal is, in part, supported by the stromal compartment which is necessary for epithelium maintenance and survival (8). To investigate whether stromal/epithelial interactions could be involved in the development of enlarged VP ducts and increased accumulation of SBP, we generated chimeric recombinant prostates derived from embryonic WT or *lxrα*$^{-/-}$ UGM and WT or *lxrα*$^{-/-}$ UGE. After recombination, the four UGE/UGM combinations (UGE_{WT}/UGM_{WT}; $UGE_{lxr\alpha-/-}/UGM_{lxr\alpha-/-}$; $UGE_{WT}/UGM_{lxr\alpha-/-}$; $UGE_{lxr\alpha-/-}/UGM_{WT}$) were grafted under the kidney capsule of nude mice (24). Eight weeks after grafting, the four types of recombinants had grown and presented a similar gross morphology characterized by differentiated prostatic lobes with enlarged tubules filled by accumulated secretions (Fig. 7A). *Ar* transcript accumulation was not altered in the different genotypes combinations. *Sbp* mRNA accumulation was strongly increased (767-fold accumulation) in the $UGE_{lxr\alpha-/-}/UGM_{lxr\alpha-/-}$ compared with the UGE_{WT}/UGM_{WT} recombinants (Fig. 7B). This showed that this phenotype was intrinsically prostatic because the recombinants were grafted in WT nude mice.

Interestingly, *Sbp* accumulation, the marker of the BPH-like phenotype, was not significantly altered when the mutant UGM was combined with the WT UGE or when the mutant UGE was combined with the WT UGM (Fig. 7B). This demonstrated that *sbp* deregulation originates from combined stromal and epithelial *lxrα*$^{-/-}$ ablation. In contrast, *Spp1* expression was deregulated when Lxrα was deleted in the epithelium alone or in combination with the mesenchyme. However, in the mesenchyme alone, Lxrα ablation had no effect on *Spp1* expression. We therefore concluded that Lxrα played a physiological role in both the stroma and epithelium. We further showed that the contribution of one or the other compartment to the phenotype was gene specific.

Discussion

In this report we show that a BPH-like phenotype of *lxrα*$^{-/-}$ mice is characterized by increased secretory activity of the epithelium. Our work using UGE/UGM recombinations provides evidence that Lxrα is involved both at the stromal and the epithelial levels. Indeed, androgen-regulated gene expression is deregulated alternatively by *lxrα* ablation in both compartments. Using *lxrα*$^{-/-}$ mice, we found that neither androgen levels in prostate, nor AR recruitment in targeted-sequences was

altered. It can thus be concluded that the observed deregulation of androgen signaling in prostate results from a complex paracrine network between the epithelium and stroma.

Lxrα and Lxrβ play an important role in prostate epithelium homeostasis in other lobes, specifically when the mice are challenged with a high-cholesterol diet (Pommier *et al.*, submitted data). As already mentioned, the human and murine prostates are architecturally different. Nevertheless, the gene expression pattern of the peripheral and central zones in human is closely related to the murine dorsolateral and ventral lobes, respectively (37). These observations highlight that the molecular signature of regionalization in the prostate is an important process conserved between the two species. Given that each lobe harbors specific features, it could be hypothesized that *lxr*α ablation results in a different phenotype according the prostate lobes *in vivo*. Consistent with our findings, *lxr*$\alpha^{-/-}$ mice have been described to recapitulate "several BPH-like features" according to Kim *et al.* (17). These authors reported fibrous nodules, abnormal stroma growth, and lesions in the muscular compartment (17), whereas we mainly reported an epithelial phenotype. This apparent discrepancy could be due to the fact that the *lxr*$\alpha^{-/-}$ strains were not similarly engineered (18, 38).

The main function of the prostate epithelium is the production and the secretion of proteins that compose prostatic fluid. This secretion activity is tightly regulated *in vivo* by androgens that orchestrate the entire male genital tract capacity. A possible connection between LXR and AR has been previously suggested. DHT or synthetic androgen R1881 treatments result in decreased *abca1* accumulation in LNCaP cells (39), indicating that LXR target genes are sensitive to androgen stimulation. Krycer and Brown (15) showed that LXR were indeed required for the *abca1* down-regulation in response to R1881 treatment. The association between the expression of LXR target genes and androgen sensitivity has also been described in xenograft models that recapitulate pharmaco-resistant prostate cancer (40). In these tumors, *fas*, *srebp1c*, *abca1*, and *cyp-27* gene expressions decrease during androgen insensitivity evolution. Interestingly, another partner of retinoid X receptor, the pregnane X receptor (NR1I2) has been demonstrated to inhibit androgen-dependent proliferation of LAPC-4 cells (41). This raises the question whether LXR and pregnane X receptor could act through a similar molecular mechanism.

Given that *lxr*α ablation resulted in an aberrant production of androgen-regulated secretory proteins in the prostate, we investigated how Lxrα could interfere with androgen signaling in the epithelium. Indeed, transgenic mice that overexpressed a dominant-positive construct of Lxrα specifically targeted in liver (42) exhibit an inhibition of androgen-dependent prostate regeneration after castration (16), indicating that Lxr activation impacts androgenic responsive tissues. Hepatic Lxrα activation leads to decreased circulating testosterone levels by regulating genes such as *sult2a1* and *sts* involved in androgen catabolism. In peripheral tissue, Lxrα controls androgens bioavailability through *sts* expression, which encodes the steroid sulfatase that desulfonates androgens to convert them into active metabolites. These data could explain the increase in testosterone levels observed in the plasma of *lxr*$\alpha^{-/-}$ mice. Nevertheless, no modification of DHT accumulation or androgen receptor activity in androgen-regulated gene promoters was seen in the VP of *lxr*$\alpha^{-/-}$ mice. Our findings indicate that the mechanism by which Lxrα regulates the response of andro-

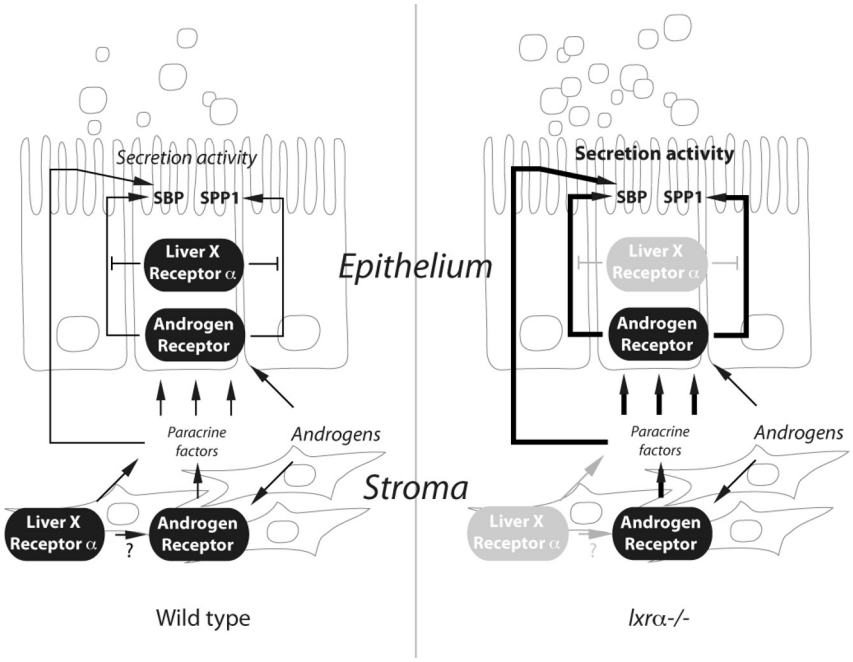

FIG. 8. Model for the physiological roles of the Lxrα in the ventral prostate and possible interactions with the androgen-regulated pathway. Schematic representation of Lxrα action in the stromal and epithelial compartments. Differential androgen-targeted genes regulation mechanisms by Lxrα are represented (*sbp* and *spp1*). *Sbp* expression is dependent of Lxrα in both the epithelium and stroma, suggesting that paracrine factors are involved. On the contrary, *spp1* expression is strictly dependent on *lxr*α expression in the epithelium. Indeed, *spp1* expression is similar to WT recombinant in the absence of Lxrα in the stromal recombinant prostates. These observations underline the multiple connections involved in the cross talk between LXR and AR.

gen-regulated genes results from a complex network. This could involve epithelial factors, AR cofactors, and/or paracrine interaction between the different cell compartments of the prostate.

Consistent with this hypothesis, androgen-regulated gene expression exhibits different profiles in $lxr\alpha^{-/-}$ mouse prostate. Although *sbp* accumulation increases in mice lacking Lxrα, *calr* remains unchanged and *pbsn* decreases. These observations strongly support that several regulatory processes are involved. We schematized the putative role of paracrine interactions between epithelial and stromal cells in Fig. 8. Prostate mesenchymal-epithelial interactions have a preponderant role in normal and pathological prostate development as well as in adult prostate homeostasis (8). The role of AR has extensively been developed in the literature (8). Here we identify Lxrα as a new actor that mediates epithelial physiology through its activity in both stroma and epithelium. Indeed, the absence of Lxrα in both prostate stroma and epithelium is necessary to develop prostate hypertrophy. Lxrα also mediates androgen signaling, as demonstrated by the numerous androgen-responsive genes dysregulated when Lxrα is missing. Indeed, normal s*pp1* gene expression needs Lxrα in epithelium, whereas the normal response of *sbp* to androgens by epithelium is dependent on Lxrα in both epithelial (directly) and stromal (indirectly) cells. The regulation of paracrine signals from the mesenchyme by lxrα might be one molecular mechanism.

Altogether these results demonstrate that Lxrα acts as a key modulator of the cross talk between the stromal and epithelial compartment, which is essential for the integration of androgen signaling in the prostate and its effect on the epithelium. Finally, identification of the set of genes targeted by Lxrα specifically in the prostatic ventral lobe in mice could be informative in understanding the BPH etiology in humans.

Acknowledgments

We thank Dr. M. Thomsen (Institute of Cancer Research, London, UK) for his excellent advices on prostate regeneration; Dr. M. Manin (GReD) for her helpful comments for the MPE cell culture; J. P. Saru and A. De Haze for molecular biology technical assistance; C. Puchol and S. Plantade for animal facilities. Dr. P. Val (GReD) and Dr. S. Ingersoll (Georgia State University, Atlanta GA) for critically reading the manuscript; and the members of the Chester's laboratory for assistance in animal dissections and discussions; C. Szczepaniak and C. Blavignac (CICS platform, Clermont University) for their scientific and technical assistance in electron microscopy; Dr. B. Viguès (LMGE, Clermont-Ferrand) for helpful discussion on electron microscopy. Pan-prostate secretion antibody was a kind gift from Dr. C. Abate-Shen (Department of Medicine, Columbia University Medical Center, New York, NY). Pathology analyses have been done on the Anip@th facility platform.

Address all correspondence and requests for reprints to: Génétique Reproduction et Développement, Unité Mixte de Recherche, Centre National de la Recherche Scientifique 6293, Clermont Université, Institut National de la Santé et de la Recherche Médicale Unité 1103, 24 Avenue des Landais, BP80026, 63171 Aubière Cedex, France. E-mail: silvere.baron@univ-bpclermont.fr.

This work was supported by the Association de Recherche sur les Tumeurs Prostatiques, Ligue Contre le Cancer (Comité Allier), Fondation pour la Recherche Médicale, Fondation BNP-Paribas and the Association de Recherche Contre le Cancer, Nouveau Chercheur Auvergne research grants (to S.B.). E.V. was supported by the Région Auvergne and Fond Européen de Developpement Régional and grants from the Association de Recherche Contre le Cancer. J.D. is supportd by a Ministère de l'Education Nationale, de la Recherche et de la Technologie grant. T.E. was the recipient of an European Community Action Scheme for the Mobility of University Students (ERASMUS) exchange grant.

Disclosure Summary: E.V., T.E., J.D., A.P., S.F., J.-L.K., L.G., L.M., J.-M.L., and S.B. have nothing to declare. E.V., J.D., L.M., J.-M.L., and S.B. are employed by the Université Blaise Pascal. A.P. was employed by the Université Blaise Pascal and now by AstraZeneca. T.E. is employed by the University of Naples. S.F. is employed by the Institut National de la Recherche Agronomique.

References

1. **Madersbacher S, Haidinger G, Temml C, Schmidbauer CP** 1998 Prevalence of lower urinary tract symptoms in Austria as assessed by an open survey of 2,096 men. Eur Urol 34:136–141
2. **Gormley GJ, Stoner E, Bruskewitz RC, Imperato-McGinley J, Walsh PC, McConnell JD, Andriole GL, Geller J, Bracken BR, Tenover JS** 1992 The effect of finasteride in men with benign prostatic hyperplasia. The Finasteride Study Group. N Engl J Med 327:1185–1191
3. **Lepor H** 1990 Role of α-adrenergic blockers in the treatment of benign prostatic hyperplasia. Prostate Suppl 3:75–84
4. **Huggins C, Clark PJ** 1940 Quantitative studies of prostatic secretion: II. The effect of castration and of estrogen injection on the normal and on the hyperplastic prostate glands of dogs. J Exp Med 72:747–762
5. **Gelmann EP** 2002 Molecular biology of the androgen receptor. J Clin Oncol 20:3001–3015
6. **Heinlein CA, Chang C** 2002 Androgen receptor (AR) coregulators: an overview. Endocr Rev 23:175–200
7. **Bruchovsky N, Wilson JD** 1968 The intranuclear binding of testosterone and 5-α-androstan-17-β-ol-3-one by rat prostate. J Biol Chem 243:5953–5960
8. **Cunha GR** 1973 The role of androgens in the epithelio-mesenchymal interactions involved in prostatic morphogenesis in embryonic mice. Anat Rec 175:87–96
9. **Cunha GR, Chung LW** 1981 Stromal-epithelial interactions—I. Induction of prostatic phenotype in urothelium of testicular feminized (Tfm/y) mice. J Steroid Biochem 14:1317–1324

10. **El-Hajjaji FZ, Oumeddour A, Pommier AJ, Ouvrier A, Viennois E, Dufour J, Caira F, Drevet JR, Volle DH, Baron S, Saez F, Lobaccaro JM** 2011 Liver X receptors, lipids and their reproductive secrets in the male. Biochim Biophys Acta 1812:974–981
11. **Tontonoz P, Mangelsdorf DJ** 2003 Liver X receptor signaling pathways in cardiovascular disease. Mol Endocrinol 17:985–993
12. **Volle DH, Lobaccaro JM** 2007 Role of the nuclear receptors for oxysterols LXRs in steroidogenic tissues: beyond the "foie gras," the steroids and sex? Mol Cell Endocrinol 265–266:183–189
13. **Fukuchi J, Kokontis JM, Hiipakka RA, Chuu CP, Liao S** 2004 Antiproliferative effect of liver X receptor agonists on LNCaP human prostate cancer cells. Cancer Res 64:7686–7689
14. **Pommier AJ, Alves G, Viennois E, Bernard S, Communal Y, Sion B, Marceau G, Damon C, Mouzat K, Caira F, Baron S, Lobaccaro JM** 2010 Liver X receptor activation downregulates AKT survival signaling in lipid rafts and induces apoptosis of prostate cancer cells. Oncogene 29:2712–2723
15. **Krycer JR, Brown AJ** 2011 Cross-talk between the androgen receptor and the liver x receptor: implications for cholesterol homeostasis. J Biol Chem 286:20637–205647
16. **Lee JH, Gong H, Khadem S, Lu Y, Gao X, Li S, Zhang J, Xie W** 2008 Androgen deprivation by activating the liver X receptor. Endocrinology 149:3778–3788
17. **Kim HJ, Andersson LC, Bouton D, Warner M, Gustafsson JA** 2009 Stromal growth and epithelial cell proliferation in ventral prostates of liver X receptor knockout mice. Proc Natl Acad Sci USA 106: 558–563
18. **Cummins CL, Volle DH, Zhang Y, McDonald JG, Sion B, Lefrançois-Martinez AM, Caira F, Veyssière G, Mangelsdorf DJ, Lobaccaro JM** 2006 Liver X receptors regulate adrenal cholesterol balance. J Clin Invest 116:1902–1912
19. **Manin M, Veyssiere G, Cheyvialle D, Chevalier M, Lecher P, Jean C** 1992 In vitro androgenic induction of a major protein in epithelial cell subcultures from mouse vas deferens. Endocrinology 131: 2378–2386
20. **Lobaccaro JM, Poujol N, Térouanne B, Georget V, Fabre S, Lumbroso S, Sultan C** 1999 Transcriptional interferences between normal or mutant androgen receptors and the activator protein 1— dissection of the androgen receptor functional domains. Endocrinology 140:350–357
21. **Monniaux D, Clemente N, Touzé JL, Belville C, Rico C, Bontoux M, Picard JY, Fabre S** 2008 Intrafollicular steroids and anti-mullerian hormone during normal and cystic ovarian follicular development in the cow. Biol Reprod 79:387–396
22. **Torres JM, Ortega E** 2003 Differential regulation of steroid 5α-reductase isozymes expression by androgens in the adult rat brain. FASEB J 17:1428–1433
23. **Nadaud I, Girousse C, Debiton C, Chambon C, Bouzidi MF, Martre P, Branlard G** 2010 Proteomic and morphological analysis of early stages of wheat grain development. Proteomics 10:2901–2910
24. **Sun Q, Yu X, Degraff DJ, Matusik RJ** 2009 Upstream stimulatory factor 2, a novel FoxA1-interacting protein, is involved in prostate-specific gene expression. Mol Endocrinol 23:2038–2047
25. **Magee JA, Chang LW, Stormo GD, Milbrandt J** 2006 Direct, androgen receptor-mediated regulation of the FKBP5 gene via a distal enhancer element. Endocrinology 147:590–598
26. **Lukacs RU, Goldstein AS, Lawson DA, Cheng D, Witte ON** 2010 Isolation, cultivation and characterization of adult murine prostate stem cells. Nat Protoc 5:702–713
27. **Cunha GR, Lung B** 1978 The possible influence of temporal factors in androgenic responsiveness of urogenital tissue recombinants from wild-type and androgen-insensitive (Tfm) mice. J Exp Zool 205: 181–193
28. **Hirota Y, Kuronita T, Fujita H, Tanaka Y** 2007 A role for Rab5 activity in the biogenesis of endosomal and lysosomal compartments. Biochem Biophys Res Commun 364:40–47
29. **Economides KD, Capecchi MR** 2003 Hoxb13 is required for normal differentiation and secretory function of the ventral prostate. Development 130:2061–2069
30. **Chaurand P, DaGue BB, Ma S, Kasper S, Caprioli RM** 2001 Strain-based sequence variations and structure analysis of murine prostate specific spermine binding protein using mass spectrometry. Biochemistry 40:9725–9733
31. **Fujimoto N, Akimoto Y, Suzuki T, Kitamura S, Ohta S** 2006 Identification of prostatic-secreted proteins in mice by mass spectrometric analysis and evaluation of lobe-specific and androgen-dependent mRNA expression. J Endocrinol 190:793–803
32. **Kawano N, Yoshida M** 2007 Semen-coagulating protein, SVS2, in mouse seminal plasma controls sperm fertility. Biol Reprod 76:353–361
33. **Seenundun S, Robaire B** 2007 Time-dependent rescue of gene expression by androgens in the mouse proximal caput epididymidis-1 cell line after androgen withdrawal. Endocrinology 148:173–188
34. **Sharief FS, Mohler JL, Sharief Y, Li SS** 1994 Expression of human prostatic acid phosphatase and prostate specific antigen genes in neoplastic and benign tissues. Biochem Mol Biol Int 33:567–574
35. **Zhu N, Pewitt EB, Cai X, Cohn EB, Lang S, Chen R, Wang Z** 1998 Calreticulin: an intracellular Ca++-binding protein abundantly expressed and regulated by androgen in prostatic epithelial cells. Endocrinology 139:4337–4344
36. **Johnson MA, Hernandez I, Wei Y, Greenberg N** 2000 Isolation and characterization of mouse probasin: an androgen-regulated protein specifically expressed in the differentiated prostate. Prostate 43: 255–262
37. **Berquin IM, Min Y, Wu R, Wu H, Chen YQ** 2005 Expression signature of the mouse prostate. J Biol Chem 280:36442–36451
38. **Alberti S, Schuster G, Parini P, Feltkamp D, Diczfalusy U, Rudling M, Angelin B, Björkhem I, Pettersson S, Gustafsson JA** 2001 Hepatic cholesterol metabolism and resistance to dietary cholesterol in LXRβ-deficient mice. J Clin Invest 107:565–573
39. **Fukuchi J, Hiipakka RA, Kokontis JM, Hsu S, Ko AL, Fitzgerald ML, Liao S** 2004 Androgenic suppression of ATP-binding cassette transporter A1 expression in LNCaP human prostate cancer cells. Cancer Res 64:7682–7685
40. **Chuu CP, Hiipakka RA, Kokontis JM, Fukuchi J, Chen RY, Liao S** 2006 Inhibition of tumor growth and progression of LNCaP prostate cancer cells in athymic mice by androgen and liver X receptor agonist. Cancer Res 66:6482–6486
41. **Zhang B, Cheng Q, Ou Z, Lee JH, Xu M, Kochhar U, Ren S, Huang M, Pflug BR, Xie W** 2010 Pregnane X receptor as a therapeutic target to inhibit androgen activity. Endocrinology 151:5721–5729
42. **Uppal H, Saini SP, Moschetta A, Mu Y, Zhou J, Gong H, Zhai Y, Ren S, Michalopoulos GK, Mangelsdorf DJ, Xie W** 2007 Activation of LXRs prevents bile acid toxicity and cholestasis in female mice. Hepatology 45:422–432